Spontaneous Inactivation of Human Tryptase Involves Conformational Changes Consistent with Conversion of the Active Site to a Zymogen-like Structure†

Trevor Selwood,‡ Darrell R. McCaslin,§ and Norman M. Schechter*,‡,||

Department of Dermatology and Department Biochemistry and Biophysics, University of Pennsylvania, Philadelphia, Pennsylvania 19104, and Department of Biochemistry, University of Wisconsin, Madison, Wisconsin 53706

Received April 7, 1998; Revised Manuscript Received June 25, 1998

ABSTRACT: The conformational changes accompanying spontaneous inactivation and dextran sulfate (DS) mediated reactivation of the serine protease human tryptase were investigated by analysis of (i) intrinsic fluorescence, (ii) inhibitor binding, and (iii) catalytic efficiency. Spontaneous inactivation produced a marked decrease in fluorescence emission intensity that was reversed by the addition of DS. Fluorescence decreases at high (4.0 μM) and low (0.1 μM) tryptase concentrations were similar at early times and coincided with loss of enzymatic activity but deviated significantly from activity loss at later times by showing a difference in the extent of change. The fluorescence losses were best described by a two-step kinetic model in which the major decrease correlated to activity loss ($t_{1/2}$ of 4.3 min in 0.2 M NaCl, pH 6.8, 30 °C) and was followed by a further decrease ($t_{1/2} \approx 60$ min) whose extent differed with tryptase concentration. The ability to bind the competitive inhibitor *p*-aminobenzamidine was reversibly lost upon spontaneous inactivation, providing evidence for conformational changes affecting the major substrate binding site (S1-pocket). Estimation of catalytic efficiency using an active site titrant showed that the specific activity of tryptase remained unchanged upon inactivation and reactivation. Return of enzymatic activity, intrinsic fluorescence, and the S1 pocket appeared to occur in the same time frame ($t_{1/2} \approx 3$ min). These studies indicate that spontaneous inactivation involves reversible changes which convert the active site to a nonfunctional state. The association of activity loss with an intrinsic fluorescence decrease and loss of the S1-pocket is consistent with the disruption of a critical ionic bond at the active site. Formation of this ionic bond is the basis of zymogen activation for the chymotrypsin family of serine proteases.

Human tryptase is a serine class protease with trypsin-like specificity. Unlike other members of this class, it is functionally unstable (*1*−*3*) rapidly losing activity via a nonproteolytic process we have termed spontaneous inactivation (*2*, *4*). The rate of activity loss is dependent on salt concentration, pH, temperature, and the binding of highly sulfated polysaccharides such as heparin or DS.[1] At 37 °C, pH 6.8, 0.2 M NaCl, the half-life for inactivation is approximately 1 min while at 4 °C, pH 6.8, 2.0 M NaCl, the enzyme is stable for weeks. Interaction of active tryptase with highly sulfated polysaccharides greatly slows spontaneous inactivation (*1*−*3*), and the addition of heparin or DS to inactivated tryptase rescues the enzyme, demonstrating the reversibility of the inactivation process (*2*−*4*).

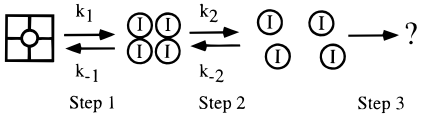

FIGURE 1: Schematic model of tryptase spontaneous inactivation. Squares denote the active tetramer species, and circles with the letter I denote inactive species. The question mark denotes an irreversibly inactivated form of tryptase that is not well characterized.

Kinetic and physical studies have helped to define intermediates and structural changes depicted in our model of spontaneous inactivation shown in Figure 1 (*2*, *4*). Tryptase purified from tissues under stabilizing conditions (e.g. high salt concentration, 4 °C) is catalytically functional and is a tetramer of four active subunits (*4*−*7*). After transfer to nonstabilizing conditions, reversible and irreversible structural changes produce a rapid and slow phase of activity loss (*2*, *4*). The rapid phase generates greater than 80% of the activity loss in a process that appears insensitive to tryptase concentration and is associated with a reversible structural change as measured by CD. To account for these properties, the first step of spontaneous inactivation (step 1) is depicted as a conformational isomerization to an inactive-

† This work was supported by NIH Grant AR42931 and Training Grant AR07465 awarded to the Department of Dermatology, University of Pennsylvania. T. S. is presently supported by the Allergan Inc. Research Fellowship awarded by the Dermatology Foundation.

* Address correspondence to this author. E-mail: schechte@mail.med.upenn.edu.

‡ University of Pennsylvania, Department of Dermatology.

§ University of Wisconsin, Department of Biochemistry, Biophysics Instrumentation Facility.

|| University of Pennsylvania, Department of Biochemistry and Biophysics.

[1] Abbreviations: CBZ, *N*-carbobenzoxy; CD, circular dichroism; DS, dextran sulfate; L-BAPNA, *N*α-benzoyl-L-arginine-NA; MOPS, 3-(*N*-morpholino)propanesulfonic acid; MUGB, 4-methylumbelliferyl 4-guanadinobenzoate; 4-MU, 4-methylumbelliferone; NA, 4-nitroanilide; NPGB, 4-nitrophenyl 4′-guanadinobenzoate; pAb, *p*-aminobenzamidine; SDS−PAGE, sodium dodecyl sulfate polyacrylamide gel electrophoresis; TOS, *N*-*p*-toluenesufonyl; TRIS, tris(hydroxymethyl)aminomethane.

S0006-2960(98)00780-6 CCC: $15.00
Published on Web 08/29/1998

destabilized tetramer. Step 2 is depicted as the dissociation of the destabilized tetramer. This step is implied by the dependence of DS/heparin-mediated reactivation on the concentration of tryptase and ultracentrifugation analysis of spontaneously inactivated tryptase that revealed an equilibrating tetramer−monomer mixture. Step 3 is the slow irreversible decay of the system which is not well characterized but is apparent from the reduced ability to rescue tryptase after long periods of incubation.

The CD spectrum of tryptase displays a rarely observed negative peak at 230 nm (*4*) that also is seen in the spectrum of chymotrypsin (*8*−*10*) but is not a general characteristic of serine proteases (*10*−*12*). This peak is lost during the fast phase of spontaneous inactivation (*4*) and also is absent in the spectra of the catalytically inactive forms of chymotrypsin: chymotrypsinogen and high-pH inactivated chymotrypsin (*8, 9*). The lack of the 230 nm peak in these inactive forms of chymotrypsin correlates to the absence of a critical ionic bond between the α-amino group of Ile^{16} and the β-carboxyl group of Asp^{194} (*8*). This bond modulates the activity of a serine protease (chymotrypsin family) in that its formation produces structural rearrangements in the active site (formation the S1 binding pocket and oxyanion hole) that dramatically enhance catalytic activity (*13*−*16*). The generation of the ionic bond after cleavage of an X-Ile^{16} bond in serine proteases is the basis of zymogen activation (*17*). In view of the similar CD characteristics of tryptase and chymotrypsin, we have suggested that step 1 in the model (Figure 1) involves the disruption of an homologous ionic bond (Ile^1−Asp^{193} in tryptase (*7*)) and reversible conversion of the active site in each tryptase subunit to a zymogen-like structure (*4*).

The peak at 230 nm in the CD spectrum of chymotrypsin has been attributed to the ellipticity of certain Trp residues which undergo a change in environment upon zymogen activation and high-pH inactivation. Initially Trp^{141} near the Ile−Asp salt bridge was believed responsible for the signal (*18*). A more recent analysis examining the possibility of exciton coupling between aromatic residues suggests that an interaction between Trp^{215} and Trp^{172} produces the signal (*19*). Tryptase has comparable aromatic residues at homologous positions which could reproduce the chymotrypsin CD signal. Chymotrypsin exhibits a change in intrinsic fluorescence upon inactivation/activation consistent with a the change in the environment of a Trp residue(s) (*20*−*22*). Although the origin of the fluorescence emission change is controversial, four of the eight Trp residues in chymotrypsin including Trp^{141} form a cluster close to Ile−Asp ionic bond (*22, 23*). Seven of nine Trp residues in human tryptase are homologous to those in chymotrypsin, including the cluster close to the Ile−Asp ionic bond (*24*−*26*). Trp residues were not in the 6 loops forming subunit interfaces in the recent X-ray crystal structure of the tryptase tetramer, suggesting that they are part of the core structure homologous to other serine proteases (*7*).

Given the similar CD properties and the extent of homology between chymotrypsin and tryptase with respect to Trp residues, we pursued our analogy to chymotrypsin in this study by examination of tryptase's intrinsic fluorescence properties. In addition, a more direct assessment of active site structure upon spontaneous inactivation was made using the fluorescent competitive inhibitor pAb (*27*) and the fluorescent active site titrant MUGB (*28*). The former was used to assess the state of the S1 pocket and the latter catalytic efficiency.

EXPERIMENTAL PROCEDURES

Materials. Dextran sulfate (8000 average molecular weight) and model substrates were purchased from Sigma. Tryptase was purified from human skin as previously described (*4*) except that the purified enzyme was dialyzed overnight at 4 °C against 2.0 M NaCl, 10 mM MOPS (pH 6.8) before concentration to 40 μM and storage at −70 °C.

Standard Assay of Tryptase and Estimation of Concentration. The standard assay conditions were 0.2 M NaCl, 0.1 M Tris-HCl (pH 8.0), 9% Me_2SO, 25 °C containing either 1.0 mM CBZ-Gly-Pro-Arg-NA, 1.0 mM TOS-Gly-Pro-Lys-NA, or 1.0 mM L-BAPNA. The K_m values for these substrates are 1.0, 1.0, and 4.0 mM, respectively. Typically assays were performed in a 1 mL volume using a semi-microcuvette of 1 cm path length. The concentration of tryptase reported in experiments represents subunit concentration. Concentrations were estimated from initial rates of product (NA) formation using specific activities for various substrates. Different substrates were employed depending on the tryptase concentration in experiments. The specific activities for CBZ-Gly-Pro-Arg-NA, TOS-Gly-Pro-Lys-NA, and L-BAPNA under standard conditions are 5.7, 3.3, and 0.20 (μmol min^{-1})(nmol of tryptase)$^{-1}$, respectively, where $\epsilon_{410\ nm}$ for NA is 8800. These specific activities were based on the concentration of tryptase active sites determined using the active site titrant MUGB (see below). Total tryptase protein concentration was estimated using the reported $\epsilon_{280\ nm}$ of 77 000 M^{-1} cm^{-1} (*6*). Comparison of concentration estimated by enzymatic activity with that obtained by protein determination (assuming 27.5 kDa for the mass of a subunit) suggested that preparations of tryptase were at least 80% active. Analysis of tryptase by SDS−PAGE (not shown) indicated that the preparations were >90% pure, and gel filtration analysis of tryptase in the presence of heparin showed only tetramer (*29*).

Initial velocity of substrate hydrolysis was measured for 3 min. Product formation was linear during this time period indicating that spontaneous inactivation of tryptase was negligible in the assay. Stability over the 3 min period was due to the lower temperature of the activity assay ($t_{1/2}$ inactivation = 25 min at 25 °C compared to 3 min under standard decay conditions) and the additional stabilizing effect of substrate binding (*4*).

Spontaneous Inactivation and Reactivation. Except for the study with the active site titrant which utilized plastic micro-centrifuge tubes for incubations, tryptase inactivations (decays) and reactivations (returns) were performed in quartz cuvettes in a solution volume of 1 mL. Spontaneous inactivation was initiated by dilution of stock tryptase (stabilized at 4 °C in 2.0 M NaCl) to standard inactivation conditions of 0.2 M NaCl, 10 mM MOPS (pH 6.8), 30 °C. As a control, the same dilution was made into a stabilizing solution of either 2.0 M NaCl, 10 mM MOPS (pH 6.8), 30 °C or 1.0 mg/mL DS, 10 mM MOPS (pH 6.8), 30 °C. The activity of the stabilized controls immediately after dilution (0-time) was used as the reference in calculating the fraction of tryptase activity remaining in decays and produced in

returns. All decay time−courses extrapolated back to the 0-time point of the control further indicating the accuracy of our measurements with regards to activity loss. Reactivation of spontaneously inactivated tryptase was performed at 25 °C and was initiated by addition of a concentrated solution of DS (50 mg/mL) to give a final concentration of 1.0 mg/mL.

Tryptase activity was monitored by withdrawing aliquots from the incubations and diluting 25−500-fold into standard assay conditions. Aliquots removed from incubations were of sufficient size to produce a hydrolytic rate of approximately 0.1 ΔA_{410}/min in the assay assuming no loss of activity. Initial velocities were determined as described above. The enzymatic activity of controls was in proportion to the dilution (typically from 40 μM tryptase to 4.0 or 0.1 μM), irrespective of the stabilizing solution employed (high salt or DS). This indicates that dilutions were quantitative and that our assays (see above) measure accurately the enzymatic activity of tryptase present in solutions that contain or do not contain a polysaccharide stabilizer.

We used DS previously to establish the CD spectrum of tryptase because it demonstrated less ellipticity than heparin in the wavelength range of interest (*4*). To be consistent with these previous studies, we continued to use DS for stabilization and reactivation. The final concentration of DS in reactivations was 1 mg/mL. At this concentration of DS or heparin (5000 kDa), the extent of return is somewhat better than observed previously using 0.1 mg/mL of heparin *(2)*. Alter et al. (*30*) had shown that DS could effectively substitute for heparin in stabilizing tryptase enzymatic activity.

Fluorescence Instrumentation. All fluorescence measurements were performed using a Perkin-Elmer 512 fluorescence spectrophotometer thermostated by means of a circulating water bath (±0.5 °C). Data were collected via an amplifier purchased from University of Pennsylvania Bioanalytical Instrumentations Group. The analogue signal from the amplifier was digitized using a MacAdios II Jr A/D converter, and data were collected using the program Superscope IIe (GW Instruments). The emission monochromator of the fluorometer was calibrated using the standard spectrum for Trp in water as published by Permyakov (*31*). The excitation monochromator was calibrated by measurement of light scattering of a dilute agarose solution (*32*).

Measurement Of Intrinsic Fluorescence. Except for the difference in the sensitivity setting, intrinsic fluorescence measurements at high and low tryptase concentration were recorded identically with excitation at 295 nm, and excitation and emission bandwidths of 10 mm; the cuvette path length was 1 cm. Emission spectra were scanned at a rate of 2 nm/s and data acquired every 0.5 s. Each data point was the average of 1000 readings collected over a 0.03 s interval. Samples were irradiated only during acquisition of the spectra (~1 min/spectrum). Photobleaching was not evident as evidenced by the constancy of the emission spectra of controls. Furthermore, the decrease in emission intensity during decays was not affected by the number of spectra taken, nor did the decrease differ when monitored at a single emission wavelength which dramatically reduced the time of irradiation (<5 s for a single reading). A small inner filter effect was observed at high tryptase concentration where the A_{295} was 0.2. The effect should not influence the analysis of the data because protein concentration was constant in each decay and reactivation, as well as controls used for comparative purposes (see below). In low concentration decays and returns a small Raman peak, less than 5% of the sample fluorescence, was subtracted from the spectra.

Emission spectra of decays at high and low tryptase concentrations were compared by displaying them relative to the 0-time spectra of controls containing an equivalent concentration of tryptase in 2.0 M NaCl. The fluorescence intensity of the control at 331 nm was assigned a value of 1. Controls were performed in parallel with all experiments. Data presented as single wavelength values were most often obtained from spectra.

The intensity-averaged emission wavelength, [λ], was calculated from emission spectra using eq 1, where I is emission intensity at each wavelength (λ_i) (*33, 34*). [λ] was obtained as a function of time for decays at high and low tryptase concentration.

$$[\lambda] = \frac{\sum_{i=1}^{N}(I_i\lambda_i)}{\sum_{i=1}^{N}(I_i)} \quad (1)$$

MUGB. Quantification of active sites was accomplished using MUGB as previously described (*35*). Aliquots (5 μL) from incubations were withdrawn and immediately added to 1 mL of 0.1 M veronal buffer (pH 8.0), 25 °C containing 0.1 mM MUGB in a cuvette. Samples were excited at 365 nm (20 nm bandwidth), and the magnitude of the burst of 4-MU product was quantified by fluorescence emission at 445 nm (20 nm bandwidth). Product concentration was estimated from standard curves obtained with either NPGB-calibrated trypsin or 4-MU. Both calibration curves were similar within experimental error.

pAb. The interaction of pAb with tryptase was studied by measurement of the fluorescence enhancement of pAb upon binding to the protease (*27*). Emission spectra were recorded in a 1 cm path length cuvette with 325 nm excitation and a band-pass of 3 nm for both excitation and emission. The dissociation constant (K_d) for interaction of pAb with tryptase was determined from plots of the fluorescence increase as a function pAb concentration, as previously described for trypsin and thrombin (*27*).

Analysis of Kinetic Data. Rate constants for enzymatic activity loss and intrinsic fluorescence changes were determined by fitting the data to a single or double exponential function ($f(t)$) according to eqs 2 or 3, respectively. In these

$$f(t) = k_0 + k_1 e^{-k_2 t} \quad (2)$$

$$f(t) = k_0 + k_1 e^{-k_2 t} + k_3 e^{-k_4 t} \quad (3)$$

equations, k_2 and k_4 are the rate constants of first-order processes and k_1 and k_3 are the magnitudes of the change for each process. All fits were performed by nonlinear least-squares regression using the program Igor Pro by Wavemetrics. All errors were expressed as standard deviations.

Table 1: Spontaneous Inactivation and DS-Mediated Reactivation of Human Tryptase[a]

	% initial activity			
	0.1 μM tryptase		4.0 μM tryptase	
decay time, h	activity loss	return after DS addition	activity loss	return after DS addition
0	100[b]		100	
0.33	13 ± 5 ($n = 5$)[c]	25 ± 1 ($n = 3$)	16 ± 3 ($n = 10$)	71
2	6 ± 2 ($n = 3$)	18 ± 4 ($n = 2$)	7 ± 2 ($n = 7$)	80 ± 12 ($n = 3$)
4	2 ± 1 ($n = 3$)		5 ± 1 ($n = 4$)	
24	1 ± 1 ($n = 3$)	16 ± 2 ($n = 2$)	5 ± 2 ($n = 4$)	55 ± 10 ($n = 2$)
48	0	15	2	60

[a] Decays were initiated by dilution of stock tryptase to the desired concentrations and conditions, 0.2 M NaCl, 10 mM MOPS (pH 6.8), 30 °C. At the times indicated, return was initiated by adjusting the incubation to 25 °C (except 20 min return which was remained at 30 °C) and addition of DS. Return values reported are based on the recovery of activity after 1−2 h in DS at 25 °C or 30 °C when most, if not all, of the return is complete. [b] 100% is the activity at 0-time for stock tryptase diluted to the desired concentration in stabilizing solution of either 2.0 M NaCl, 10 mM MOPS (pH 6.8) or 0.2 M NaCl, 10 mM MOPS (pH 6.8), 1.0 mg/mL DS (controls). At 0-time, the activity of both stabilized controls was identical. After 48 h, the DS control lost less than 10% of its activity while the high salt control lost approximately 70% of its activity. [c] The number of determinations (n) is given in parentheses; values reported without errors (SD) are from single determinations.

Kinetic Simulation of the Fluorescence Loss. The kinetic simulation program Hopkinsim (D. H. Wachsstock and T. P. Pollard, Johns Hopkins Medical School) was used to analyze the kinetics of the fluorescence loss according to a two step model comprised of steps 1 and 2 in Figure 1, where the entire fluorescence decrease was attributed to step 2 (dissociation). In this simulation, loss in activity, step 1 in Figure 1, was treated as an approach to an equilibrium in which 85% of the tryptase is inactive; that is [inactive]/[active] $= k_1/k_{-1} = 5.7$ and the observed rate constant (0.16 min^{-1}) for activity loss is the sum of $k_1 + k_{-1}$ (*36*). Step 2 was assigned the association equilibrium constant (K_a) of 5×10^{15} M^{-3} estimated by sedimentation equilibrium ultracentrifugation (*4*). k_2 was assigned various rate constants, and k_{-2} was assigned the value of $K_a k_2$. The values of k_2 ranged from 0.01 to 0.16 min^{-1}, the high value being the rate constant for activity loss. At the high value, the simulation fit the fluorescence loss at early times, but the decrease was much too fast to be compatible with the data at later times. Reducing the magnitude of k_2 produced a lag phase at early times which was not observed experimentally.

RESULTS

Spontaneous Inactivation At High And Low Tryptase Concentrations. Both intra- and intersubunit changes may affect the intrinsic fluorescence of tryptase upon spontaneous inactivation. To investigate the contribution of each, spontaneous inactivation was studied at 0.1 and 4.0 μM tryptase. These concentrations provide a range where the extent of tetramer dissociation after inactivation is predicted to differ (*4*). Tetramer is predicted to be about 50% dissociated at the high concentration (50% of the subunits are monomeric) and virtually completely dissociated at the low concentration.

In Table 1, loss and return of enzymatic activity are reported for decays of 0.1 and 4.0 μM tryptase under standard conditions. Decays were initiated by dilution of stock tryptase as described in Experimental Procedures. As previously shown (*2*, *4*), both decays revealed a biphasic loss of fractional activity with approximately 85% of the enzymatic activity lost after 20 min followed by a slower loss of the remaining activity. The fraction of activity lost during the first 20 min and at least up to 2 h was similar at each tryptase concentration. Upon continued incubation small differences in residual activity were observed. In contrast to the loss of fractional activity, the extent of reactivation produced by addition of DS differed in each decay with the high concentration incubation exhibiting a greater extent of return than the low concentration incubation.

The ability to recover tryptase enzymatic activity in each decay by DS addition remained relatively constant through 48 h of incubation. The relative constancy of the return over 48 h of incubation suggests that step 3 (Figure 1), the irreversible decay of the system, is not having a major influence on inactivation. The stability of the system over the time of incubation reported here is better than previously reported in our initial study (*4*). The reasons for the better stability of the system have not been systematically evaluated. The reduced influence of the irreversible step implies that it is primarily of a nonspecific nature.

Specific Activity of Tryptase During spontaneous Inactivation and Reactivation. Previously we had shown that loss of tryptase enzymatic activity was related to a loss of functional active sites (*2*). A time-course to evaluate the specific activity of tryptase during spontaneous inactivation and DS-mediated reactivation is shown in Figure 2. Reactivation was initiated by addition of DS to the incubation after 100 min of decay. Active site concentration was monitored using MUGB, an active site titrant, and enzymatic activity was determined by L-BAPNA hydrolysis; both determinations are expressed on a fractional basis in the figure. The parallel change in both measurements indicates that the specific activity of tryptase (enzymatic activity/active site concentration) is unchanged during both inactivation and reactivation processes. This finding demonstrates that spontaneous inactivation and DS-mediated reactivation involve the loss/gain of catalytic subunits rather than a change in the specific activity of all subunits. This result further supports the reversibility of spontaneous inactivation as denoted by steps 1 and 2 in Figure 1.

Intrinsic Fluorescence of Active Tryptase. Normalized fluorescence emission spectra of active tryptase at 4.0 and 0.1 μM tryptase stabilized in 2.0 M NaCl are shown in Figure 3 (control spectra); excitation was at 295 nm. Both spectra appeared similar in shape and revealed an emission maximum of 331 nm. Fluorescence spectra of tryptase stabilized in

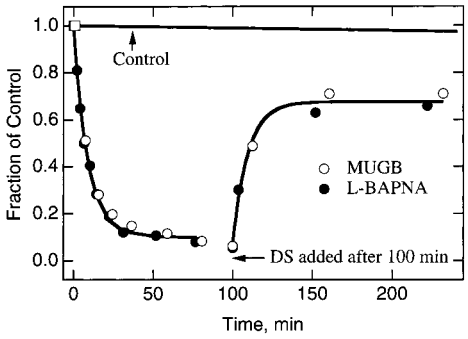

FIGURE 2: Parallel loss/gain of enzymatic activity and active site concentration upon spontaneous inactivation and DS-mediated reactivation. Data are expressed as a fraction of the control. A 500 μ L mixture containing 4.0 μM tryptase under decay conditions of 0.2 M NaCl, pH 6.8, 30 °C was periodically assayed either for enzymatic activity with L-BAPNA or for active site concentration with MUGB as described in Experimental Procedures. Reactivation was initiated after 100 min under decay conditions. At this time the incubation was cooled to 25 °C (5 min) and DS was added. The sample was periodically assayed as before. The control line (squares) is for DS-stabilized tryptase monitored for activity and active site concentration. Little change in both controls was observed over 24 h of incubation as indicated by the line.

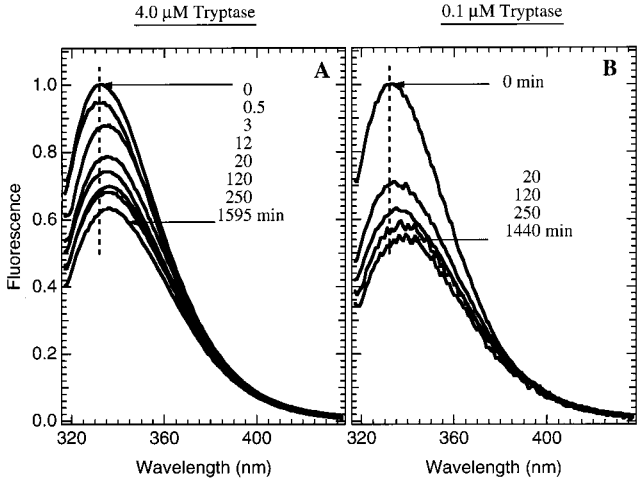

FIGURE 3: Change in the intrinsic fluorescence spectrum of tryptase upon spontaneous inactivation at high (A) and low (B) concentrations. Tryptase at each concentration was decayed in the cuvette under conditions of 0.2 M NaCl, pH 6.8, 30 °C. The 0-time spectra are 4.0 and 0.1 μM tryptase in 2.0 M NaCl stabilizing conditions. The dashed vertical line marks the 331 nm emission maximum of active tryptase.

DS−0.2 M NaCl were similar in shape to those in 2.0 M NaCl, except that the emission intensity was reduced by approximately 15%. The lower intensity is likely due to quenching brought about by the interaction of DS with tryptase. Consistent with this interpretation, dissociation of DS from tryptase by increasing the NaCl concentration to 2.0 M reproduced the high salt spectrum. Tryptase contains 9 Trp and 10 Try residues (*24*−*26*) which may contribute to its spectrum. Spectra obtained by excitation at 280 nm did not show a shoulder at 310 nm (not shown), indicating that Trp residues were the major source of the emission (*31*, *32*).

Intrinsic Fluorescence Spectrum of Tryptase during Spontaneous Inactivation. All emission spectra measured during spontaneous inactivation under decay conditions (0.2 M NaCl, pH 6.8, 30 °C) are reported relative to the 0-time point

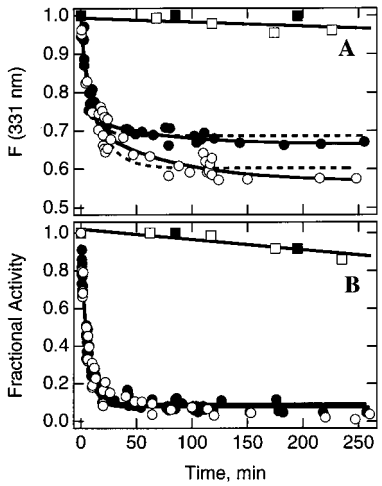

FIGURE 4: Time-courses for fluorescence emission (A) and enzymatic activity (B) loss upon the spontaneous inactivation of tryptase. Inactivation conditions are the same as reported in Figure 3. Relative emission intensity at 331 nm is reported in panel A, and fractional activity loss is reported in panel B. Open and closed boxes are controls of tryptase at each concentration in 2.0 M NaCl. Open and closed circles are decays at 0.1 and 4.0 μM tryptase, respectively. Dashed lines in panel A and solid lines in panel B were obtained by fitting the data to a single-exponential function (eq 2). Solid lines panel A were obtained by fitting a data to a double exponential function (eq 3). Data producing each time-course were obtained from several independent experiments.

of a control incubation (2.0 M NaCl, pH 6.8, 30 °C) at an identical concentration of tryptase. Validating the use of the control, normalized spectra of controls at 0.1 and 4.0 μM did not significantly change over the 250 min of incubations (331 nm data in Figure 4A). Spectra also were unaffected by the 10-fold reduction in the NaCl concentration. This is evidenced by the spectrum obtained in 0.2 M NaCl after 0.5 min of inactivation (Figure 3) which is identical to that of 2.0 M NaCl control, except for a slight loss of intensity resulting from spontaneous inactivation.

Spectra recorded during spontaneous inactivations at high and low tryptase concentrations are shown in Figure 3A,B. In both decays there is a significant decrease in intrinsic fluorescence relative to stabilized tryptase. Except for the greater extent of decrease in the low concentration decay, spectra at corresponding times have a similar shape and reveal a progressive shift in the emission maximum from 331 to 335 nm upon inactivation. Difference spectra determined by subtracting the 20 or 250 min spectra from that of the 2.0 M NaCl (0-time) exhibited a maximum at 328 nm (data not shown). The decrease in intensity and shift to a longer maximum wavelength is consistent with an increase in the quenching of the fluorescence of Trp residue(s). The maximum at 328 nm for the difference spectra is consistent with the loss of fluorescence of an internal (buried) Trp residue(s) (*31*).

Spectra of decays at high and low tryptase concentration also were evaluated by calculating the intensity-averaged emission wavelength ([λ] in eq 1) which is more sensitive to spectral shifts than the emission maximum (*33*, *34*). The results of this calculation suggested that the low concentration decay slowly progressed to a slightly longer wavelength than the high. [λ] of active tryptase at both high and low concentration was 345.6 $\pm$ 0.1 nm. Upon inactivation [λ] shifted to a final value of 348.8 $\pm$ 0.3 nm in the high

Table 2: Results Obtained by Fitting Fluorescence Data to Eq 3[a]

tryptase, μM	k_0	k_1[b]	k_2, min^{-1}	k_3	k_4, min^{-1}
0.1[a]	0.56 ± 0.03	0.26 ± 0.03	0.16 ± 0.03	0.16 ± 0.03	0.014 ± 0.006
4.0	0.66 ± 0.01	0.26 ± 0.03	0.16 ± 0.03	0.07 ± 0.03	0.01 ± 0.01

[a] Analysis by a double exponential function yielded preexponential (k_1) and rate constants (k_2) for the rapid phase of the fluorescence loss and preexponential (k_3) and rate constants (k_4) for the slow phase of fluorescence loss; k_0 is the fluorescence at infinite time. [b] Fitted variables k_1 and k_2 were constrained to be identical at both concentrations.

concentration decay and 349.8 ± 0.2 nm in the low concentration decay. These values are the average (±SD) of several spectra taken between 3 and 24 h of decay when further change was no longer evident. The emission maximum and [λ] of inactivated tryptase is less than that observed for proteins in strong denaturing agents such as urea and guanidine hydrochloride, suggesting that inactivated tryptase is not fully unfolded (*33, 34*).

Kinetics of Intrinsic Fluorescence Changes. The time-courses for the intrinsic fluorescence decrease over a 250 min period of spontaneous inactivation at high and low tryptase concentration are shown compared to fractional activity loss in Figure 4A,B, respectively. The fluorescence emission intensity at 331 nm and enzymatic activity are plotted relative to the control (squares) at 0-time. The most striking difference in comparing the two sets of decreases is the effect of tryptase concentration on the fluorescence loss. The 0.1 μM decay revealed a significantly greater extent of fluorescence loss than the 4.0 μM tryptase decay (Figure 4A). This concentration effect was not apparent in the fractional activity loss (Figure 4B). The time-courses for fluorescence and activity losses were empirically fit to eq 2 (dashed lines in Figure 4A) in order to compare the rates of decrease. The $t_{1/2}$ values for the fluorescence decreases in the high and low concentration decays were 5.8 and 11.6 min (rate constants 0.12 ± 0.01 and 0.06 ± 0.01 min^{-1}), respectively, compared to 4.3 min (rate constant 0.16 ± 0.01 min^{-1}) for the activity decrease at both concentrations.

The disparity between the fluorescence emission and activity time-courses support the multistep model for spontaneous inactivation as depicted in Figure 1. Although the simplest interpretation for the concentration dependence and relative slowness of the fluorescence decrease is to associate the fluorescence loss entirely with step 2 (dissociation), this possibility was discounted on the basis of several observations: (i) An initial lag in the fluorescence loss which might support such a possibility was not detected. (ii) A significant difference in the extent of dissociation should have been mirrored in the fractional activity loss, as increased dissociation (95% complete by 1 h assuming the $t_{1/2}$ above) should favor formation of inactive species. (iii) The single-exponential fit (eq 2) underestimates the extent of loss at later times (compare dashed lines vs data points in Figure 4A). (iv) A time-course consistent with the fluorescence data could not be reproduced using a kinetics simulation program to predict the rate of dissociation according to the model in Figure 1 (see Experimental Procedures). In regards to the last observation, the magnitudes of k_2 and k_{-2} for the dissociation equilibrium (step 2) required to make the simulation fit the data at early times produced completion of the simulation much earlier than the data. In fact, the simulation indicated that the fluorescence loss at early times was occurring at the same rate as activity loss. The inability to attribute the fluorescence data to step 2 exclusively along with its correspondence with activity loss at early times suggested that both steps 1 and 2 were contributing to the fluorescence changes.

The fluorescence data at high and low concentration were analyzed further using a double exponential function (eq 3) to describe the time-courses. When the fluorescence data sets were fit individually to eq 3, the rate constants (k_2) and preexponential factors (k_1) describing the kinetics of the initial fluorescence decrease were found to be nearly identical at each concentration, consistent with the concentration independence observed for activity loss. Thus data for high and low concentrations of tryptase were merged and fit to a model in which these constants (k_1 and k_2) were constrained to be identical for both data sets, and the other rate constant (k_4), preexponential factor (k_3), and the values for fluorescence at infinite time (k_0) were allowed to differ with tryptase concentration. As shown by the solid lines in Figure 4A and values in Table 2, the data were well represented by this model. The rate constant independent of tryptase concentration was virtually identical to that obtained for activity loss ($t_{1/2}$ of 4.3 min) indicating that the fluorescence loss at early times was attributable to events concomitant with the fast phase of activity loss. The rate constants obtained for the other exponential decay were much smaller than that of the first decay, predicting a slow process with a $t_{1/2}$ in the range of 1 h.

The sums of the preexponential terms and the infinite time fluorescence for both high and low concentration decays were nearly unity confirming that the model accounted for all of the fluorescence present at time zero. While the model constrains the preexponential term for the common fast rate to be the same at high and low tryptase concentrations, the fraction that this process contributes to the overall change in fluorescence is dependent on the tryptase concentration with the fast process contributing 80% and 60% of the total fluorescence change at high and low concentrations, respectively. This is consistent with a fixed portion of the total fluorescence change coming from the fast phase of inactivation and a concentration dependent fraction arising from the slow dissociation of inactive tetramers.

Fluorescence Emission Changes upon Reactivation. The reversibility of the intrinsic fluorescence loss was investigated in decays at high and low tryptase concentration. Reactivation was initiated after 120 min of decay by addition of DS, and emission spectra were recorded as a function of time. Return of activity and fluorescence at each concentration was virtually complete after 1 h of incubation, at which time the high and low concentration decays returned activity to 80% and 23% of the initial activity, respectively. In Figure 5, the emission spectra of tryptase recorded immediately before and 1 h after addition of DS are shown, as well as spectra of active tryptase stabilized by DS for comparison. In

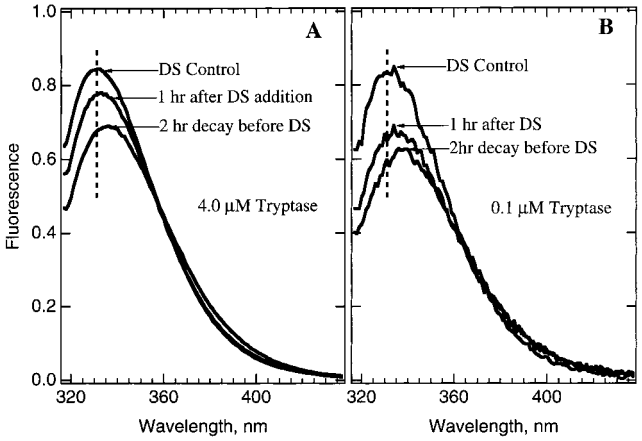

FIGURE 5: Recovery of intrinsic fluorescence upon DS-mediated reactivation of decays performed at high (A) and low (B) concentration tryptase. Each decay was for 120 min at 30 °C in a cuvette. The incubation was then cooled to 25 °C and DS was added; spectra immediately before and 1 h after DS addition are shown. The dashed vertical line marks the emission maximum of active tryptase at 331 nm. The DS control is of an equivalent concentration of tryptase stabilized from the outset of incubation by the presence of DS.

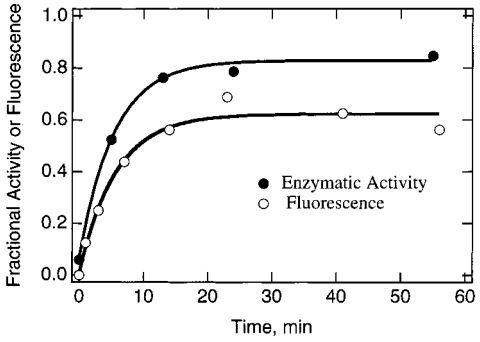

FIGURE 6: Rate of return of enzymatic activity and intrinsic fluorescence upon addition of DS to spontaneously inactivated tryptase. Inactivation of 4.0 μM tryptase (to 5% of its initial activity) and reactivation was initiated as described in Figure 5. At the indicated times, the intensity of the fluorescence emission at 331 nm was determined with excitation at 295 nm. Also periodically 5 μL aliquots were removed from the cuvette for activity assay using L-BAPNA. Conversion of fluorescence to a fractional quantity is described in the text. The solid lines were obtained fitting each data set to eq 2.

qualitative agreement with the extent of the activity returns, the spectrum of reactivated high-concentration tryptase looked more similar in intensity and shape (emission maximum returned close to 331 nm) to the spectrum of the DS control than that of reactivated low-concentration tryptase. Spectra of the DS controls changed very little over the course of the incubation.

The rates of return of enzymatic activity and fluorescence intensity for the reactivation of 4.0 μM tryptase are compared in Figure 6. Fluorescence emission intensity is expressed on a fractional scale where 1 is the intensity of DS-stabilized tryptase and zero is the intensity of inactivated tryptase immediately before the addition of DS. Analysis of both data sets empirically using eq 2 revealed a similar rate of return; $t_{1/2}$ values of 3.6 and 3.8 min (rate constants = 0.19 $\pm$ 0.02 and 0.18 $\pm$ 0.03 min^{-1}) were measured for activity and fluorescence return, respectively.

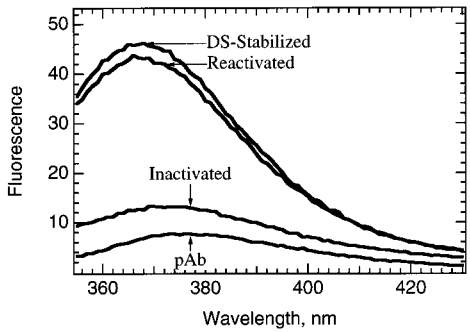

FIGURE 7: Binding of pAb to DS-stabilized, inactivated and reactivated tryptase. Emission spectra were recorded as described in Experimental Procedures. In all measurements the pAb concentration was 40.0 μM and the tryptase concentration was 4.0 μM, except for the control of pAb alone. Tryptase is 60% saturated in the presence of 40.0 μM pAb. Stabilizing conditions were 1.0 mg/mL DS, 0.2 M NaCl, pH 6.8, and 30 °C (DS-stabilized). The spectrum of pAb with inactivated tryptase was obtained at 25 °C after decay of the enzyme for 120 min in 0.2 M NaCl, pH 6.8, 30 °C in the absence of pAb (inactivated). To obtain the spectrum of pAb with reactivated tryptase, DS was added to inactivated tryptase just described and the spectrum was obtained after 30 min of incubation at 25 °C (reactivated).

In Figure 6, the extent of the fluorescence return appears less than that of the activity return. The reason for this difference is unclear. It may reflect the absence of an appropriate baseline value to quantify fluorescence on a fractional scale. Quenching of the emission intensity in the decayed sample due to DS interaction with the remaining active tryptase or upon binding to inactivated species would reduce the baseline value below that of zero used in our calculation. Nevertheless, the above studies suggest that intrinsic fluorescence changes during spontaneous inactivation are reversible and closely correlate with loss/gain of enzyme activity.

Reversible Loss of the S1 Pocket during Spontaneous Inactivation. pAb is a competitive inhibitor of serine proteases with trypsin-like specificity. Interaction of pAb with tryptase has been reported to have a K_i of 19 μM (*37*). pAb binds reversibly to the S1 pocket (*27, 38, 39*), and burial within this pocket enhances the fluorescence emission of pAb providing a spectroscopic method for measurement of binding (*27*). The fluorescence enhancement of pAb bound to enzymatically active tryptase is demonstrated in Figure 7, where the spectra of 40.0 μM pAb in the presence 4.0 μM tryptase reveals a shift in the emission maximum from 376 to 366 nm and a significant enhancement in emission intensity. The intensity increase at 376 nm was approximately 80-fold for pAb bound to tryptase compared to free pAb. A similar change in pAb fluorescence has been reported for the interaction with trypsin and thrombin (*27*). By utilization of the enhancement of pAb fluorescence, a dissociation constant (K_d) of 21 μM for the interaction pAb with DS-stabilized tryptase was determined. Addition of an excess of leupeptin (200 μM, K_i = 1.5 μM), another competitive inhibitor of tryptase, to a solution of pAb−tryptase complex reduced the fluorescence intensity to near background levels (data not shown). This characterization strongly suggests that the fluorescence enhancement produced by the interaction of pAb with tryptase is the result of burial within the S1 pocket.

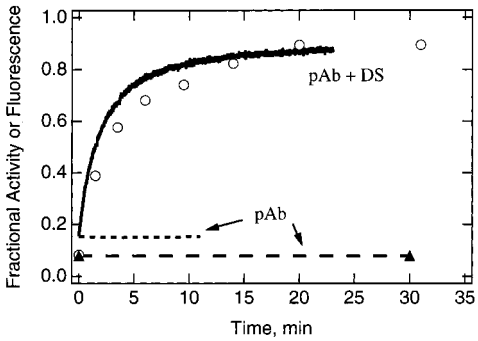

FIGURE 8: Rate of return of enzymatic activity and pAb binding upon reactivation of tryptase. Tryptase at 4.0 μM was inactivated in 2 cuvettes for 120 min at 0.2 M NaCl, pH 6.8, 30 °C. At this time both incubations were cooled to 25 °C and pAb was added to a concentration of 40 μM. Fluorescence emission and activity were recorded at this time to establish a 0-time point. To one incubation, DS was added to a final concentration of 1.0 mg/mL to produce reactivation. Fluorescence emissions of both samples were then monitored continually at 376 nm with 325 nm excitation. The solid and short dashed lines represent incubations with and without DS, respectively. Periodically a 5 μL aliquot was removed and assayed for activity with L-BAPNA. Open circles and triangle−long dashes represent incubations with and without DS, respectively. To overcome the inhibitory effect of pAb in enzymatic assays, 5 μL aliquots were diluted 100-fold with assay solution. Fractional activity and fluorescence are plotted versus time. To convert fluorescence to a fractional quantity a scale was established where 1 is the emission intensity of 40.0 μM pAb in the presence of tryptase stabilized by DS from the outset and 0 is the emission intensity of pAb alone (not shown).

Fluorescence spectra demonstrating the interaction of 40.0 μM pAb with 4.0 μM tryptase after 120 min of spontaneous inactivation and after return of activity by addition of DS also are shown in Figure 7. The spectrum of pAb observed with inactivated tryptase shows a marked reduction in the degree of enhancement compared to that observed with DS-stabilized tryptase, consistent with reduced pAb binding upon spontaneous inactivation. The small enhancement is likely due to the 8% active enzyme remaining and some nonspecific background fluorescence. Reactivation of the same incubation by addition of DS returned the enhancement almost to the magnitude of the control. The return of fluorescence intensity is consistent with the return of activity measured at 90% of initial activity by enzymatic assay. Thus changes in the integrity of the S1 pocket upon spontaneous inactivation are reversible.

The time-courses for both the return of enzymatic activity (circles) and pAb binding upon reactivation (solid line) are shown in Figure 8. Reactivation was initiated by sequential addition of pAb and DS. Return of fluorescence was monitored continuously except for brief interruptions when aliquots were removed to assay enzymatic activity. To estimate the rate of return of each parameter, recoveries were fit to eq 2. The $t_{1/2}$ values obtained from the fits were 2.3 and 3.0 min for pAB binding and activity return, respectively. The similarity of the values suggests that changes to the S1 pocket are closely linked to activity loss/gain. The rate of loss of pAb fluorescence was not compared to activity loss because near saturating levels of the inhibitor dramatically decreased the rate of tryptase inactivation. This stabilizing effect is similar to that previously reported for the inhibitor, leupeptin (*4*). pAb added to inactivated tryptase in the absence of DS did not produce a return in activity or fluorescence (dashed lines).

DISCUSSION

This study further defines the structural changes producing the spontaneous inactivation of tryptase. We have shown previously that the spontaneous inactivation of tryptase is a biphasic process. The initial phase is rapid, accounts for the major portion of enzymatic activity loss, and is not affected by tryptase concentration (*2*). The second phase is the slow continuation of the activity loss. Structural studies have related the kinetics of activity loss primarily to reversible intra- (step 1) and inter- (step 2) subunit structural changes as depicted in Figure 1 (*4*). An irreversible process (step 3) was included in the model to account for changes that affect the DS/heparin mediated reactivation of tryptase after long periods of decay. The relatively small difference in the extent of reactivation over the decay period of 48 h as shown in Table 1 suggests that step 3 was not significantly affecting the results of our studies which were primarily obtained over the first 250 min of incubation.

Two other studies of spontaneous inactivation have been reported recently which suggest that activity loss proceeds through the formation of an inactive-tetramer intermediate (*3, 40*). Both models of inactivation reported in these studies differ from ours and from each other in the nature and reversibility of the species resulting from inactivation. One suggests that reactivation by heparin produces a monomeric species with a lower specific activity than that of a tetrameric subunit, while the other suggests that the reassociation of monomers to the active tetramer is a pH-dependent process that does not require heparin. Results in the present study provide further support for the simple reversibility of steps 1 and 2 in our model. Analysis of the specific activity of tryptase upon spontaneous inactivation and after DS-mediated reactivation demonstrated no change in this value (Figure 2), indicating that active enzyme produced by reactivation is the same as that isolated from tissues. The reactivation of 0.1 μM tryptase after 24−48 h of decay, where we predict the sample to be completely monomeric (*4*), suggests that monomers can reassociate to form the active tetramer. The difference in the extent of the return in the 4.0 and 0.1 μM decays (Table 1) confirms the concentration dependence of the reactivation process shown previously (*2*) and not considered in the other models. These properties along with the tetramer−monomer equilibrium indicated by sedimentation equilibrium analyses of inactivated tryptase (*4*) support the concept that the species resulting from spontaneous inactivation are in equilibrium and that reactivation by DS or heparin is produced by the influence of these polysaccharides on this equilibrium.

The CD spectra of active and inactivated tryptase differ in the region of 230 nm. A similar difference in the spectra of chymotrypsin and chymotrypsinogen has led us to postulate that spontaneous inactivation involves structural changes which convert tryptase to a zymogen-like form; i.e., a form in which the Ile−Asp ionic bond, S1 pocket, and oxyanion hole of the active site are disrupted (*13−16*). Because the origin of the CD signal may be aromatic residues (*18, 19*) and chymotrypsin displays an increase in intrinsic fluorescence upon zymogen activation (*20−22*), we explored

further our analogy by investigating tryptase intrinsic fluorescence. In addition, active site structure was more directly probed using a competitive inhibitor which binds to the S1 pocket.

Spontaneous inactivation was accompanied by a marked decrease in fluorescence emission intensity which was relatively greater in decays at 0.1 μM than 4.0 μM tryptase. As shown in Results, the kinetics of the emission loss were best described as biphasic, exhibiting a fast and slow phase analogous to activity loss. Using a double exponential model to analyze the data, the rate constant for the fast phase of the fluorescence decrease observed at both high and low tryptase concentration was identical to that observed for activity loss ($t_{1/2}$ = 4.3 min) and accounted for 80% of the fluorescence decrease at the high concentration and about 60% at the low. The fluorescence decreases were reversed by addition of DS in a manner consistent with the recovery of activity. The correlation of the fast phase of activity loss with a reversible fluorescence decrease suggests that structural changes involving Trp residues are associated with a process insensitive to tryptase concentration. This observation supports our analogy with chymotrypsin and further defines the structural nature of step 1 in our model (Figure 1).

A decrease in tryptase intrinsic fluorescence during spontaneous inactivation has been reported in another study (*3*) and was attributed totally to the dissociation of an inactive-tetramer intermediate. As only one concentration of tryptase (1 μM) was investigated and data were obtained at large time intervals (based on the one time-course presented), it is possible that the biphasic nature of the decays was not apparent in this study. In the same study fluorescence anisotropy, a technique sensitive to protein dissociation, suggested a half-time for dissociation of 22 min. In our analysis, the fluorescence decrease associated with the slow phase accounted for the concentration dependence of the fluorescence data. Supporting this assumption, the "intensity-averaged emission wavelength" of spectra taken at later times in the decay indicated a slightly greater red shift for low concentration tryptase decay than the high. The half-life for the slow phase of the fluorescence loss was 60 min, a value considerably longer than that obtained for the fast phase. Considering the error in the measurement, this value may be compatible with that obtained by fluorescence anisotropy. A slow dissociation step is compatible with the concentration independence we find for the fast phase of activity loss and the biphasic nature of the inactivation kinetics.

The recent crystal structure of tryptase demonstrates that the tetrameric form of tryptase is a square-planer structure with a sizable central pore (*7*). Significantly Trp residues were not present at the subunit interfaces, suggesting that a large change in intrinsic fluorescence could occur independent of dissociation. The structure further revealed that the interface regions producing the tetramer consisted of symmetrical contacts between sets of loops that have adopted conformations specific for docking. The specificity of these contacts suggests that dissociation may not be a simple one-step process.

Whereas fluorescence and CD provide indirect evidence for structural changes at the active site, a more direct measurement was made using the competitive inhibitor, pAb, which binds to the S1 pocket (27, 38, 39). In serine proteases, the S1 pocket is a cavity that binds the side chain of the residue on the carbonyl side of scissile bond. The architecture of the cavity determines the general substrate specificity of the protease (chymotrypsin-, trypsin-, elastase-like), and the functionality of this pocket is generally determined by the formation/disruption of the Ile−Asp ionic bond. Analysis of the interaction of pAb with tryptase revealed a dramatic reduction in the binding of pAb upon spontaneous inactivation which was reversed by addition of DS. This finding suggests that the integrity of the S1 pocket was reversibly altered by spontaneous inactivation and provides a further basis for associating spectral changes and activity loss with disruption of the Ile−Asp ionic bond and conversion of tryptase to a zymogen-like structure.

The major structural changes associated with activation of a serine protease zymogen occur in a relatively specific region of the protease termed the activation domain (*41*). Measurement of the kinetics of these structural changes in α-chymotrypsin suggests that the active-zymogen transformation is a cooperative process (*42*, *43*). Within the experimental error of our studies, intrinsic fluorescence and S1 pocket changes during spontaneous inactivation/reactivation appear to correlate with activity, suggesting that they are produced by a single or cooperative process associated with activity loss/gain. Previously we reported that the CD change produced by spontaneous inactivation coincided with activity loss upon inactivation but appeared to return somewhat more rapidly than activity upon reactivation (*4*). This was based on our best estimate of the rate of activity return at this time. The average of many more reactivations since this study suggest a somewhat faster rate ($t_{1/2}$ of 3 vs 10 min) of activity return better correlating the CD change with activity.

The ionic nature of the Ile−Asp bond also confers pH sensitivity to the structure/function of a serine protease in addition to that arising from the catalytic His residue. This sensitivity is typically observed as an apparent pK_a for the reversible loss of activity in the alkaline pH range (*8*, *42*, *43*). Most serine proteases exhibit apparent pK_a's for activity loss greater than 8.5. Since this value is above the pK_a of an α-amino group (8.0) in solution, protein structure is believed to contribute to the stability of the Ile−Asp ionic bond (*42*−*44*). In α-chymotrypsin, the contribution of protein structure to the ionic bond's stability is relatively weak, and at neutral pH where the α-amino group is fully protonated, only 85% of the enzyme is in the active form in equilibrium with 15% of the enzyme in the zymogen-like form (*42*, *43*). On the basis of our interpretation of spectral and S1 pocket changes during spontaneous inactivation, we suggest that the fast phase of spontaneous inactivation is the attainment of a similar equilibrium for tryptase subunits established while in the tetrameric form (step 1 in Figure 1). In the case of tryptase, the equilibrium ratio of inactive "zymogen-like" to active subunits is approximately the reverse of the chymotrypsin values (85% zymogen-like, 15% active).

What makes the Ile−Asp bond unusually weak in tryptase subunits compared to other serine proteases? More than likely, structural elements in addition to those classically involved in the activation/inactivation of chymotrypsin (*13*, *15*) and trypsin (*14*) have a role. The relative slowness of

the spontaneous inactivation process which exhibits $t_{1/2}$ values in the range of minutes compared to less than 1 s for α-chymotrypsin (*42*, *43*) may be an indication of the contribution of these elements to conformational changes. These novel rearrangements may serve to "loosen" the structure of the activation domain, allowing for disruption of the Ile−Asp ionic bond by perhaps solvation of charge, and to weaken the quaternary structure of tryptase by destabilization of subunit interfaces. The structural asymmetry at one of the two subunit interfaces revealed in the tryptase crystal structure may be indicative of stress which is relaxed in the destabilized tetramer conformation (*7*). Identifying the tryptase-specific structural changes will be a new phase of our study.

ACKNOWLEDGMENT

We are grateful to the Pathology Department of the University of Pennsylvania and to the National Disease Research Institute (NDRI) for their help in the collection of human skin used to purify tryptase. We also thank Michele Walter for technical help and Michael Plotnick for helpful discussions. Special thanks to Dr. Fred Karush for the gift of the fluorescence spectrophotometer used in these studies and to Catherine Royer for advice on the analysis of fluorescence data.

REFERENCES

1. Schwartz, L. B., and Bradford, T. R. (1986) *J. Biol. Chem. 261*, 7372−7379.
2. Schechter, N. M., Eng, G. Y., and McCaslin, D. R. (1993) *Biochemistry 32*, 2617−2625.
3. Addington, A. K., and Johnson, D. A. (1996) *Biochemistry 35*, 13511−13518.
4. Schechter, N. M., Eng, G. Y., Selwood, T., and McCaslin, D. R. (1995) *Biochemistry 34*, 10628−10638.
5. Schwartz, L. B., Lewis, R. A., and Austen, K. F. (1981) *J. Biol. Chem. 256*, 11939−11943.
6. Smith, T. J., Houghland, M. W., and Johnson, D. A. (1984) *J. Biol. Chem. 259*, 11046−11051.
7. Pereira, P. J. B., Bergner, A., Macedo-Ribeiro, S., Huber, R., Matschiner, G., Fritz, H., Sommerhoff, C. P., and Bode, W. (1998) *Nature 392*, 306−311.
8. McConn, J., Fasman, G. D., and Hess, G. P. (1969) *J. Mol. Biol. 39*, 551−562.
9. Sasaki, T., Kobayashi, M., and Kise, H. (1997) *Biotechnol. Techniques 11*, 387−390.
10. Wu, J., Yang, J. T., and Wu, C.-S. C. (1992) *Anal. Biochem. 200*, 359−364.
11. Rosenkranz, H. (1974) in *Bayer Symposium V, Proteinase Inhibitors* (Fritz, H., Tschesche, H., Greene, L. J., and Truscheit, E., Eds.) pp 458−462, Springer-Verlag, New York.
12. Yang, J. T., Chuen-Shang, C., and Martinez, H. M. (1986) *Methods Enzymol. 130*, 208−257.
13. Freer, S. T., Kraut, J., Robertus, J. D., Wright, H. T., and Xuong, N. H. (1970) *Biochemistry 9*, 1997−2009.
14. Fehlhammer, H., Bode, W., and Huber, R. (1977) *J. Mol. Biol. 111*, 415−438.
15. Sigler, P. B., Blow, D. M., Matthews, B. W., and Henderson, R. (1968) *J. Mol. Biol. 35*, 143−164.
16. Stroud, R. M., Kossiakoff, A. A., and Chambers, J. L. (1977) *Annu. Rev. Biophys. Bioeng. 6*, 177−193.
17. Renatus, M., Engh, R. A., Stubbs, M. T., Huber, R., Fischer, S., Kohnert, U., and Bode, W. (1997) *EMBO J. 16*, 4797−4805.
18. Cantor, C. R., and Timasheff, S. N. (1982) *The Proteins 5*, 145−305.
19. Grishina, I., and Woody, R. (1994) *Faraday Discuss. 99*, 245−262.
20. Teale, F. W. J. (1960) *Biochem. J. 76*, 381−388.
21. Kim, Y. D., and Lumry, R. (1971) *J. Am. Chem. Soc. 93*, 1003−1013.
22. Reshetnyak, Y. K., and Burnstein, E. A. (1997) *Biofizika 42*, 785−795.
23. Desie, G., Boens, N., and De Schryver, F. C. (1986) *Biochemistry 25*, 8301−8308.
24. Johnson, D. A., and Barton, G. J. (1992) *Prot. Sci. 1*, 370−377.
25. Miller, J. S., Westin, E. H., and Schwartz, L. B. (1990) *J. Clin. Invest. 86*, 864−870.
26. Vanderslice, P., Ballinger, S. M., Tam, E. K., Golstein, S. M., Craik, C. S., and Caughey, G. H. (1990) *Proc. Natl. Acad. Sci. U.S.A. 87*, 3811−3815.
27. Evans, S. A., Olson, S. T., and Shore, J. D. (1982) *J. Biol. Chem. 257*, 3014−3017.
28. Jameson, G. W., Roberts, D. V., Adams, R. W., Kyle, W. S. A., and Elmore, D. T. (1973) *Biochem. J. 131*, 107−117.
29. Wang, Z.-M., Walter, M., Selwood, T., Rubin, H., and Schechter, N. M. (1998) *Biol. Chem. 379*, 167−174.
30. Alter, S. C., Metcalfe, D. D., Bradford, T. R., and Schwartz, L. B. (1987) *Biochem. J. 248*, 821−827.
31. Permyakov, E. A. (1993) *Luminescent Spectroscopy of Proteins* pp 35−77, CRC Press, Boca Raton, FL.
32. Lakowicz, J. R. (1983) *Priciples of Fluorescence Spectroscopy* pp 341−381, Plenum, New York.
33. Royer, C. A., Mann, C. J., and Matthews, C. R. (1993) *Prot. Sci. 2*, 1844−1852.
34. Royer, C. A. (1995) *Methods Mol. Biol. 40*, 65−89.
35. Chase, T., and Shaw, E. (1970) *Methods Enzymol. 19*, 20−27.
36. Fersht, A. R. (1977) *Enzyme Structure and Mechanism* pp 103−133, W. H. Freeman and Co., San Francisco, CA.
37. Stü zebecher, J., Prasa, D., and Sommerhoff, C. P. (1992) *Biol. Chem. Hoppe-Seyler 373*, 1025−1030.
38. Bode, W., and Schwager, P. (1975) *J. Mol. Biol. 98*, 693−717.
39. Kreiger, M., Kay, L. M., and Stroud, R. M. (1974) *J. Mol. Biol.* 209−230.
40. Ren, S., Sakai, K., and Schwartz, L. (1998) *J. Immunol. 160*, 4561−4569.
41. Bode, W. (1979) *J. Mol. Biol. 127*, 357−374.
42. Fersht, A. R., and Requena, Y. (1971) *J. Mol. Biol. 60*, 279−290.
43. Fersht, A. R. (1972) *J. Mol. Biol. 64*, 497−509.
44. Hedstrom, L., Lin, T.-Y., and Fast, W. (1996) *Biochemistry 35*, 4515−4523.

BI980780C